THE JOURNAL OF BIOLOGICAL CHEMISTRY VOL. 281, NO. 8, pp. 4795–4801, February 24, 2006


# Oligomeric Structure of the Carnitine Transporter CaiT from *Escherichia coli*[*]

Received for publication, August 15, 2005, and in revised form, November 16, 2005 Published, JBC Papers in Press, December 19, 2005, DOI 10.1074/jbc.M508993200

**Kutti Ragunath Vinothkumar**[‡1], **Stefan Raunser**[‡1], **Heinrich Jung**[§], **and Werner Kühlbrandt**[‡2]

*From the* [‡]*Max Planck Institute of Biophysics, Max-von-Laue Strasse 3, D-60438 Frankfurt am Main, Germany and* [§]*Department of Biology I, Ludwig-Maximilians-Universität, D-80638 München, Germany*

**The carnitine transporter CaiT from *Escherichia coli* belongs to the betaine, choline, and carnitine transporter family of secondary transporters. It acts as an L-carnitine/γ-butyrobetaine exchanger and is predicted to span the membrane 12 times. Unlike the other members of this transporter family, it does not require an ion gradient and does not respond to osmotic stress (Jung, H., Buchholz, M., Clausen, J., Nietschke, M., Revermann, A., Schmid, R., and Jung, K. (2002) *J. Biol. Chem.* 277, 39251–39258). The structure and oligomeric state of the protein was examined in detergent and in lipid bilayers. Blue native gel electrophoresis indicated that CaiT was a trimer in detergent solution. This result was further supported by gel filtration and cross-linking studies. Electron microscopy and single particle analysis of the protein showed a triangular structure of three masses or two parallel elongated densities. Reconstitution of CaiT into lipid bilayers yielded two-dimensional crystals that indicated that CaiT was a trimer in the membrane, similar to its homologue BetP. The implications of the trimeric structure on the function of CaiT are discussed.**

The *Escherichia coli* carnitine transporter is a member of the betaine, choline, and carnitine transporter (BCCT)[3] family of secondary transporters. The BCCT family comprises a large group of membrane proteins, which share the common functional feature of transporting substrates containing a quaternary ammonium group. Most transporters of this family utilize electrochemical gradients for substrate accumulation. Some respond to osmotic stress and take up osmoprotectants, such as glycine, betaine, proline, ectoine, or trehalose (1). Sequence alignment of the proteins in the BCCT family shows two conserved regions, which are possibly involved in substrate binding. This includes a stretch of conserved residues along the putative transmembrane helices 3 and 4 and the adjacent loops. The second stretch comprises transmembrane 8 and an adjacent loop. This latter region is rich in tryptophan residues. Binding of the substrate causes a conformational change, which has been studied by analyzing tryptophan fluorescence emission in CaiT (2).

Unlike its homologue BetP, the protein sequence of CaiT shows no N- or C-terminal extensions. In BetP, these extensions are responsible for osmosensing and regulation (1). CaiT differs from the other members of this family also with respect to the use of the electrochemical gradient. It acts as an L-carnitine/γ-butyrobetaine exchanger and does not respond to osmotic stress (2). *E. coli d*ehydrates L-carnitine accumulated by CaiT. The resulting crotonobetaine is used as an electron acceptor under anaerobic conditions, which results in the end product γ-butyrobetaine (3).

Many membrane proteins have a strong tendency to associate into oligomers. The oligomeric state of a particular protein may be essential for its function, as in the case of ion channels, or simply required for stability, as in the case of porins. Secondary transporters are diverse membrane proteins, which have been found in a variety of oligomeric states, that tend to be conserved in a given family or subfamily (4). Thus sugar symporters and phosphate antiporters of the major facilitator family are monomers (5–7), whereas the ion antiporters are dimeric (8–11). A trimeric architecture has been observed in the case of AcrB (12), belonging to the root nodulation division family, in glutamate transporters (13) and in BetP of the BCCT family (1). The role of oligomers in secondary transporters is not always evident. For some, it has been shown or proposed that monomers cooperate with one another during transport (14, 15), implying that the oligomeric state is essential for function.

Knowledge of the quaternary structure is also important for structural studies; for example, crystallization requires monodisperse solutions that contain only one oligomeric state. Unfortunately, determining the quaternary structure of a membrane protein is usually not trivial. A wide variety of techniques, including genetic approaches, chemical cross-linking, analytical ultracentrifugation, size exclusion chromatography, and electron microscopy, have been used (4), but no single technique is entirely satisfactory. We have used some of these techniques to determine the quaternary structure of CaiT and discuss its implications for function.

## MATERIALS AND METHODS

*Expression and Purification of CaiT*—CaiT was expressed in *E. coli* strain BL21 plysS with either an N- or C-terminal $His_6$ tag and purified as described previously (2). For detergent exchange, dodecylmaltoside (DDM) was replaced on a nickel column with respective detergents (obtained from Anatrace or Glycon). For analytical gel filtration, a Superose 6 column (Amersham Biosciences) was used in combination with a SMART system. Blue native gel electrophoresis was carried out as described previously (16). Gel dimensions were 16 cm × 18 cm × 1 mm. Linear polyacrylamide (6–16%) gradient gels were cast with 4% overlay. For SDS dissociation and redialysis, 50 μg of protein was incubated with 0.075% SDS for 5 min and then dialyzed overnight at room temperature. The dialysis buffer contained 0.05% (w/v) DDM at pH 8.

*Cross-linking of CaiT in Detergent*—Different cross-linkers were added to 30 μg of protein in 25 mM $KP_i$, pH 7.4, 300 mM NaCl, 10% glycerol, and 0.05% DDM. Bis(sulfosuccinimidyl)succinate (Pierce) and disuccinimidyl suberate (Sigma)) were dissolved in dimethyl sulfoxide

* This work has been funded in part by the International Max-Planck Research School, "Structure and Function of Biological Membranes" and SFB 628. The costs of publication of this article were defrayed in part by the payment of page charges. This article must therefore be hereby marked "*advertisement*" in accordance with 18 U.S.C. Section 1734 solely to indicate this fact.

[1] These authors contributed equally to this work.

[2] To whom correspondence should be addressed: Dept. of Structural Biology, Max-Planck Institute of Biophysics, Max-von-Laue Str. 3, D-60438 Frankfurt am Main, Germany. Tel.: 49-69-63033000; Fax: 49-69-63033002; E-mail: werner.kuehlbrandt@mpibp-frankfurt.mpg.de.

[3] The abbreviations used are: BCCT, betaine, choline, and carnitine transporter; DDM, β-D-dodecylmaltoside; DPPC, 1,2-dipalmitoyl-*sn*-glycero-3-phosphocholine; POPC, 1-palmitoyl-2-oleoyl-*sn*-glycero-3-phosphocholine.

($Me_2SO$) and added to a final concentration of 1 and 10 mM, respectively. As a control, $Me_2SO$ was added alone. Glutaraldehyde (Agar Scientific, Stansted, UK) was added to final concentrations of 0.25, 0.5, 2.5, or 5 mM. After incubation for 30 min at room temperature, the reaction was quenched by the addition of 1/6 volume of 1 M Tris-HCl, pH 7.4. The cross-linked samples were then analyzed on 10% SDS gel stained with Coomassie Blue.

*Single Particle Analysis*—Protein was diluted to a final concentration of 0.01 mg/ml in 20 mM Tris-HCl, pH 8.0, 0.05% DDM, 10% glycerol, and 300 mM NaCl and applied to glow-discharged 400-mesh copper grids coated with a thin carbon film. The specimens were negatively stained with 1.5% uranylacetate. Electron micrographs were recorded under low dose conditions in a Philips CM120 electron microscope at 100 kV accelerating voltage and a calibrated magnification of 58,600×. Images were taken at a defocus range of 0.8–1 $\mu$m. Micrographs were digitized using a Zeiss SCAI scanner with an effective pixel size of 21 $\mu$m, corresponding to 0.36 nm on the scale of the specimen.

Single particles were selected manually from the images using the program WEB (17). The images were processed using the program SPIDER (17). Selected particles were windowed into 80 × 80 pixel boxes and normalized with the background of the electron micrograph (18). The images were centered, and a first reference was obtained by reference-free alignment (19). All particles were then aligned to this new reference using simultaneous translational/rotational algorithms based on cross-correlations of two-dimensional radon transforms (20, 21). The aligned particles were classified using pattern recognition by a neuronal network algorithm (22) of the program XMIPP (23) using a field of 7 × 7 nodes. Several nodes were selected and used as references in multireference alignments. The aligned particles were assigned to the reference for which they showed the highest cross-correlation coefficient. Neuronal network analysis and multireference alignments were repeated several times until the particles in a class converged to a homogenous population.

*Two-dimensional Crystallization*—Purified protein in DDM was reconstituted into various lipids (Avanti) at a final concentration of 1 mg/ml with varying lipid to protein ratios from 0.25 to 0.75 (w/w). The ternary mixture of protein, lipid, and detergent was incubated on ice for 1 h before dialysis. Dialysis was carried out for detergent removal against 25 mM AMPSO (3-*N*-($\alpha$-$\alpha$-dimethyl-hydroxyethyl)-amino-2-hydroxypropane sulfonic acid), pH 9, 0.25 mM NaCl, 10% glycerol, and 3 mM $NaN_3$ for 7 days at 37 °C with a molecular mass cutoff of 14 kDa.

*Electron Microscopy and Image Processing*—Two-dimensional crystals were stained with 1.5% uranylacetate. Images were recorded in a CM12 microscope operating at 120 kV in low dose mode with a magnification of 35–45,000×. Selected image areas of 4000 × 4000 pixels were digitized with a pixel size of 7 $\mu$m on a Zeiss SCAI scanner. Images were processed using the Medical Research Council image processing programs (24, 25).

## RESULTS

*Protein Purification and Blue Native Gel Electrophoresis*—Typically we obtained up to 2.5 mg of pure protein from a liter of culture. It was possible to solubilize CaiT with a number of different detergents, but the protein was stable only in those with a carbon chain length of 10 or above, with the maltoside head group preferred. The purity of the protein was >95% after a single step of nickel affinity chromatography as judged by SDS-PAGE and Coomassie staining. The protein was stable for more than a week at 4 °C in DDM without aggregation or proteolysis. The molecular mass of CaiT calculated from the amino acid sequence was ~57.4 kDa, but the apparent mass estimated by SDS-PAGE was ~36 kDa.

Blue native gel electrophoresis of CaiT indicates a band at ~250 kDa, a little above catalase, which was used as the marker, indicating that the transporter is an oligomer in detergent solution. The position of the band was not affected by the addition of substrate. The oligomer dissociated into monomers upon incubation with SDS prior to electrophore-

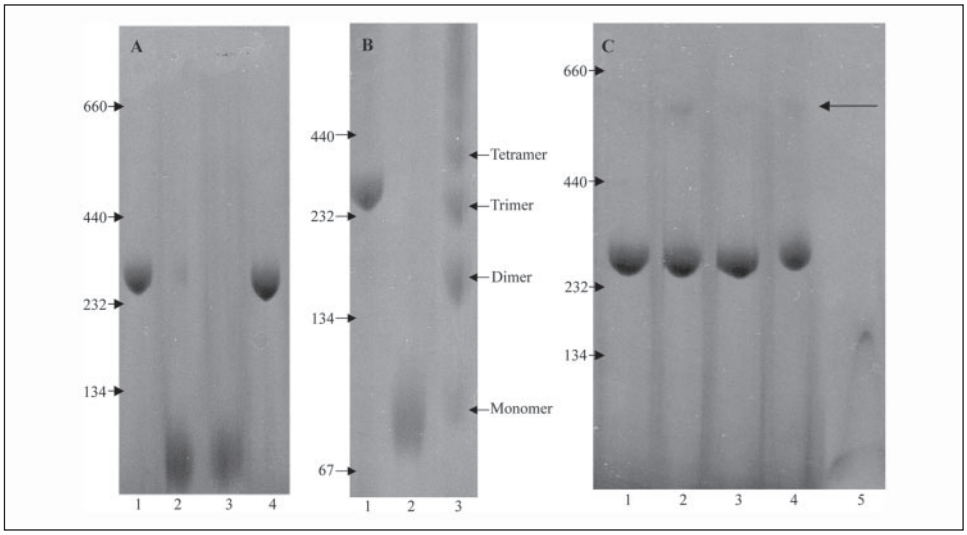


FIGURE 1. **Blue native gel electrophoresis of CaiT.** *A*, effect of SDS and substrate on the oligomeric state of CaiT. Purified protein (6 $\mu$g) in 0.05% DDM at pH 8 was mixed with gel-loading dye to a final concentration of 1× (resulting in a final Coomassie Brilliant Blue concentration of 0.5%), loaded on a gradient gel (6–16% acrylamide), and resolved at 4 °C. *Lane 1*, protein in DDM; *lanes 2* and *3*, 1 and 2% SDS added before loading on the gel; *lane 4*, protein with 25 mM carnitine. *B*, calibration of the blue native gel with an oligomer ladder of CaiT generated by SDS treatment. 50 $\mu$g of protein was incubated with 0.075% SDS for 5 min and then dialyzed overnight at room temperature in a dialysis buffer containing 0.05% (w/v) DDM at pH 8. The dialyzed protein was then analyzed by blue native gel electrophoresis. 5 $\mu$g of protein was loaded in each lane. *Lane 1*, CaiT in DDM; *lane 2*, CaiT in DDM + 0.075% SDS incubated for 5 min before loading; *lane 3*, oligomeric ladder of CaiT formed after dissociation with SDS followed by dialysis. *C*, stability of CaiT in different detergents. Membranes containing CaiT were solubilized with DDM and bound to a nickel affinity column. DDM was exchanged on the column by equilibration with buffer containing the detergent of choice at a concentration that was roughly two times its critical micelle concentration. The column was subsequently washed extensively with new detergent with 10 and 30 mM imidazole to remove impurities and DDM. The protein was eluted from the column under standard conditions, except that the elution buffer contained the respective new detergent. 5 $\mu$g of protein was loaded in each lane. *Lane 1*, protein in DDM; *lane 2*, protein in $\beta$-D-decylmaltoside; *lane 3*, protein in *n*-cyclohexyl-1-hexyl-$\beta$-D-maltoside; *lane 4*, protein in nonyl glucoside; *lane 5*, protein in zwittergent3–12. The *long arrow* indicates the formation of higher oligomers.

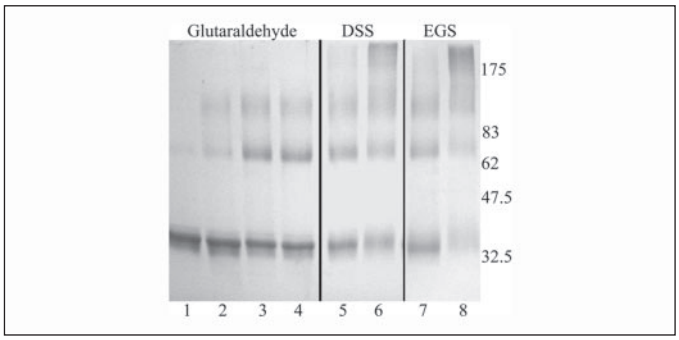


FIGURE 2. **Cross-linking of CaiT.** Protein purified in DDM (30 $\mu$g) was incubated with different cross-linkers at varying amounts for 30 min at room temperature, and the reaction was quenched with 1/6 volume of 1 M Tris-HCl, pH 7.4. The cross-linked products were resolved on a 10% polyacrylamide gel and detected by Coomassie staining. *Lane 1*, protein with no added cross-linker; *lanes 2–4*, 0.25, 0.5, and 2.5 mM of glutaraldehyde; *lanes 5* and *6*, 1 and 10 mM of disuccinimidyl suberate (*DSS*); *lanes 7* and *8*, 1 and 10 mM of bis(sulfosuccinimidyl)succinate (Sulfo-*EGS*).

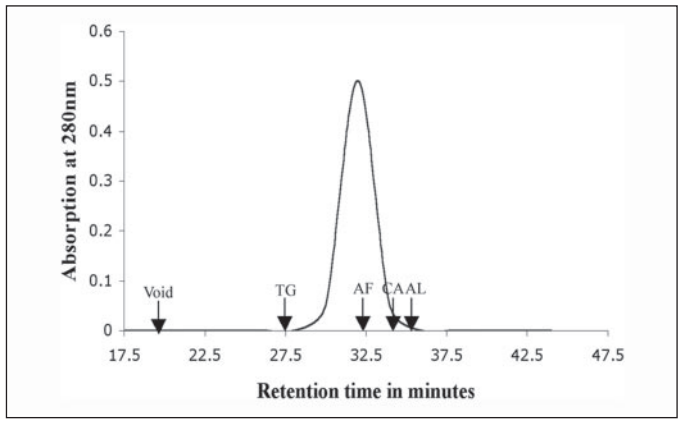


FIGURE 3. **Gel filtration profile of CaiT in DDM on a Superose 6 column.** Elution times of standard proteins of known Stokes radius are indicated: *TG*, thyroglobulin (86 Å); *AF*, apoferritin (63 Å); *CA*, catalase (52 Å); *AL*, aldolase (46 Å). 50 $\mu$g of purified protein was loaded and eluted with 0.05% DDM buffer at pH 8.

sis (Fig. 1*A*). When an SDS-treated sample was dialyzed against DDM buffer overnight, a ladder of clearly distinguished bands was observed on the blue native gel, with masses corresponding to a CaiT monomer, dimer, trimer, or tetramer. This ladder was used for estimating the apparent mass of the oligomer and indicated that CaiT is a trimer in detergent solution. The trimer was stable at pH values of from 5 to 9. At pH 4, it tended to precipitate. The CaiT trimer was not affected by a final DDM concentration up to 1.5% (data not shown).

To check the stability of the protein in different detergents, DDM was exchanged on the nickel-nitrilotriacetic acid column by equilibration with buffer containing other detergents at a concentration of two times the critical micelle concentration. A representative gel is shown in Fig. 1*C*, with protein in DDM as a positive control and zwittergent3–12 as a negative control. In detergents with a carbon chain length of 9 or 10, a higher band corresponding to a CaiT hexamer was observed (Fig. 1*C*, *lanes 2* and *4*).

*Cross-linking*—Purified protein in DDM solution was cross-linked with reagents of varying spacer lengths. When analyzed by SDS-PAGE, the control without the cross-linker migrated predominantly as a monomer at ~36 kDa, as expected. A diffuse band corresponding to a dimer was also seen (Fig. 2). With increasing concentrations of cross-linker, higher oligomeric forms of CaiT were observed. The prominent band at ~100 kDa corresponds to the trimer. At higher concentrations, small amounts of larger oligomers formed independent of the length of the cross-linker.

*Gel Filtration*—CaiT co-purifies with the lipids phosphatidylglycerol and phosphatidylethanolamine as analyzed by thin-layer chromatography (data not shown). The oligomeric state of the CaiT-lipid-detergent complex in DDM was investigated by gel filtration on a Superose 6 column calibrated with soluble proteins. The transporter eluted from the column as a single peak with a retention time of 31.5 min, indicating an apparent size of the CaiT-lipid-detergent complex corresponding to a Stokes radius of 63 Å, similar to apoferritin (Fig. 3).

*Electron Microscopy and Single Particle Analysis*—Protein purified in DDM was observed in the electron microscope as single particles. A total of 5015 particles was selected from 6 micrographs (Fig. 4*A*). After several steps of translational/rotational alignment using radon transforms and pattern recognition by neuronal networks (Fig. 4*B*), two homogenous particle classes were easily distinguished (Fig. 5, *C* and *D*). Class I contained 67.5% of the particles and showed clearly three round densities arranged in a triangle with an edge length of ~85 Å. The diameter of each density was ~38 Å. This was evidently a face-on view of a CaiT oligomer with 3-fold symmetry, either a trimer or a hexamer. Class II with 32.5% of the particles showed an arrangement of two apparently unconnected, elongated densities arranged parallel to one another. The density was weaker in the center of the elongated particles. The dimensions of the elongated particles were 85 × 43 Å. The center-to-center distance was ~27 Å. This view can be interpreted as a sandwich of two trimers seen edge-on. The resolution of the class I and II averages were calculated to be 21 and 23 Å, respectively (Fig. 5, *A* and *B*), with a cutoff criterion of five times noise correlation.

The effect of uranylacetate on the CaiT trimer was analyzed by blue native gel electrophoresis (Fig. 4*C*). A band corresponding to a CaiT hexamer was prominent at the concentrations of uranylacetate used for negative staining, indicating that the heavy metal salt promoted the association of CaiT trimers into symmetrical hexamers, presumably by charge screening of protein exposed on the membrane surface.

*Two-dimensional Crystallization*—CaiT was reconstituted with lipid into proteoliposomes in a wide pH range. At pH 7.5–9, the protein formed two-dimensional lattices in the reconstituted membranes. The two-dimensional crystals assumed different shapes, with vesicular structures predominating, but occasionally tubular crystals were observed that are frequently found with other transporters. At the low lipid to protein ratio of ~0.2 (w/w), the membranes were small and poorly ordered. The optimal lipid to protein ratio for two-dimensional lattice formation was 0.4–0.5, whereas at a higher lipid to protein ratio, the lipid vesicles tended not to contain protein, as indicated by freeze-fracture electron microscopy. The vesicular crystals showed a hexagonal lattice, and the initial crystals obtained had a tendency to stack (Fig. 6, *A* and *C*). An initial screen of lipids with different head groups and chain lengths (14 to 18) indicated that negatively charged lipids, such as phosphatidylglycerol or cardiolipin, promoted stacking. Therefore uncharged lipids were used in subsequent trials. Finally, the best two-dimensional lattices were obtained with DPPC and POPC under similar conditions. These vesicles containing the best two-dimensional lattices measured on average 0.5–1 $\mu$m (Fig. 6, *B* and *D*), but the resolution was limited to ~25 Å, as indicated by crystallographic image processing.

The unit cell of the two-dimensional crystals in isolated vesicles was $a = b = 93$ Å, $\gamma = 120°$, independent of the lipids used. The program ALLSPACE (26) indicated that isolated vesicles had 3-fold symmetry, whereas the stacked membranes exhibited higher symmetries, such as P6 and P622. Images of the isolated vesicles were merged, and a projection map at 25 Å was calculated with P3 symmetry applied (Fig. 7). The approximate dimension of the trimer calculated from the projection map was ~90 Å, and the diameter of a monomer density was ~38 Å.

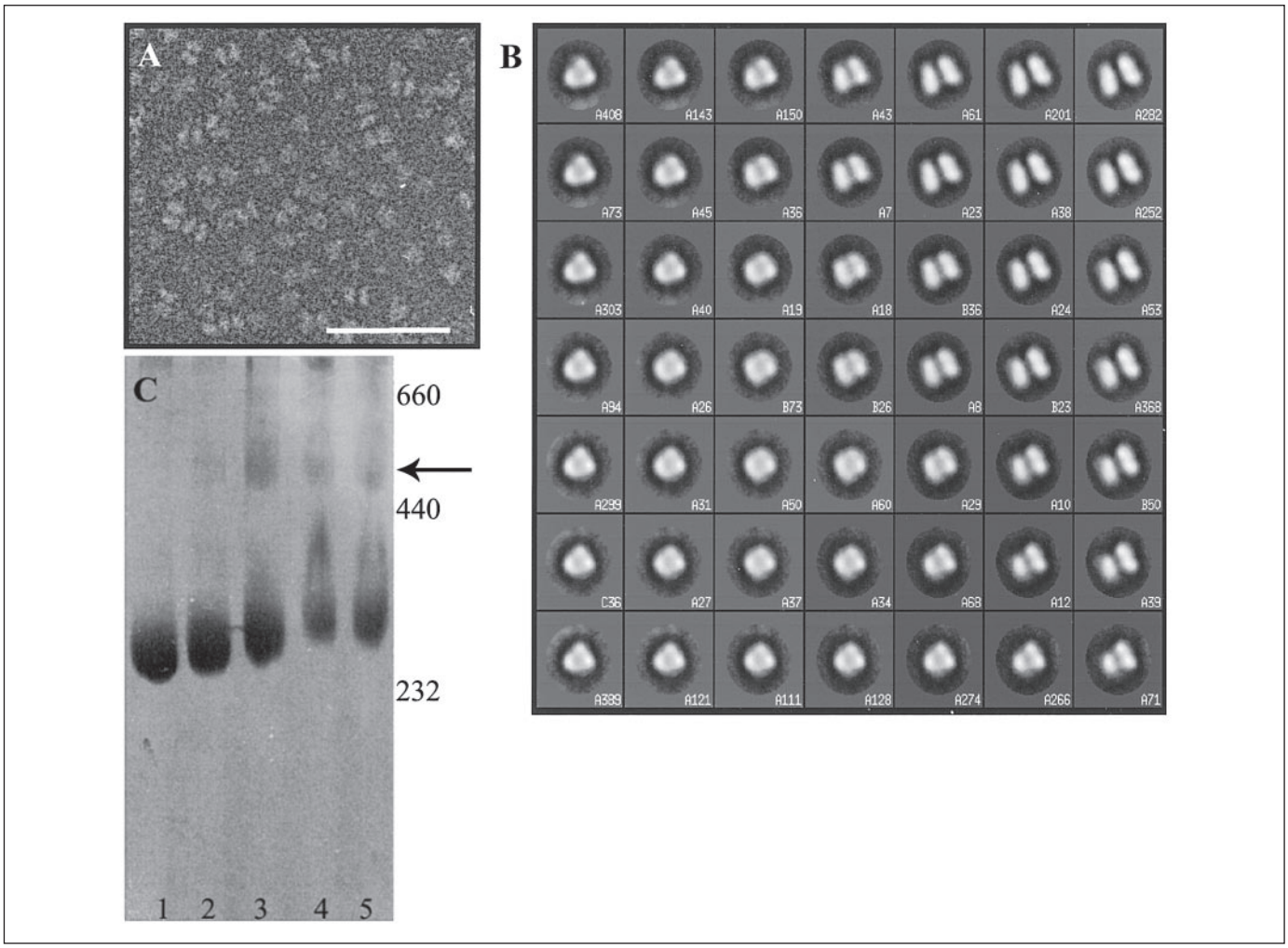


FIGURE 4. **Single particle analysis of CaiT.** *A*, electron micrograph of negatively stained CaiT. *Scale bar* is 100 nm. *B*, self-organizing map of selected averaged particles. Two node images were selected as references from an initial multireference alignment. The *numerals* indicate the number of particles in each class. *C*, blue native gel showing the effect of uranylacetate on CaiT. Protein in DDM (8 $\mu$g) was incubated with different concentrations of uranylacetate for 5 min at room temperature and subsequently loaded. *Lane 1*, protein in DDM; *lanes 2–5*, increasing concentrations of uranylacetate at 1, 2, 5, and 10 mM. The *arrow* indicates the hexamer.

## DISCUSSION

We used different methods to investigate the oligomeric structure of CaiT. Determining the exact number of subunits in an oligomeric membrane protein by biochemical or hydrodynamic means is difficult because of the presence of unknown amounts of lipids and detergent in mixed micelles. Blue native electrophoresis has been used to study the oligomeric state of membrane proteins, including LacS (27), SecYEG complex (28), and glutamate transporters (29). We observed that CaiT migrates slightly >232 kDa (Fig. 1*A*). For membrane proteins with multiple membrane-spanning helices, the molecular mass on blue native gels has been shown to be up to 1.8 times greater than predicted from the amino acid sequence (27) apparently because of bound stain. In our approach, we did not measure the amount of bound Coomassie stain. However, taking advantage of the observation that SDS dissociates the trimer into monomers, we promoted the formation of aggregates that resulted in a ladder of oligomers starting with the monomer (Fig. 1*B*). In this ladder, the band corresponding to a trimer migrates a little lower than the native protein. This may be due to bound SDS that has not been displaced by Coomassie stain.

For other transporters, such as LacS (27), an equilibrium between monomer and dimer has been observed, whereas a detergent-mediated change in the oligomeric state was found for SecYEG from *E. coli* (28). By comparison, the trimer of CaiT appears to be very stable and dissociates only upon the addition of harsh detergents, such as SDS. This stability may be due to unusually strong ionic and hydrophobic interactions between the protein monomers or to lipid-protein interactions. In fact, negatively charged lipids have been shown to be important in the stability of oligomers, such as KcsA (30) and LHCII (31). The structures of AcrB and GltPh suggest that the central region between trimers may be filled with lipids (12, 13). When purified CaiT was subjected to lipid analysis, we found both phosphatidylethanolamine and phosphatidylglycerol co-purifying with the protein. We therefore believe that the stability of the CaiT trimer is a result of lipid-protein interactions. The presence of this oligomeric state is also supported by the cross-linking results (Fig. 2).

Interpretation of the gel filtration profile of a membrane protein largely depends on the amount of bound detergent and the shape of the protein-detergent micelle. For secondary transporters with multiple membrane-spanning helices, the amount of bound DDM is in the range of 150–180 molecules/monomer, corresponding to 70–90 kDa (27). The molecular mass of the CaiT monomer calculated from the amino acid sequence is 57.4 kDa. Without bound detergent and lipid, a CaiT trimer would therefore have a molecular mass of 174 kDa, whereas the observed retention time of CaiT corresponds to ~440 kDa (Fig. 3). This

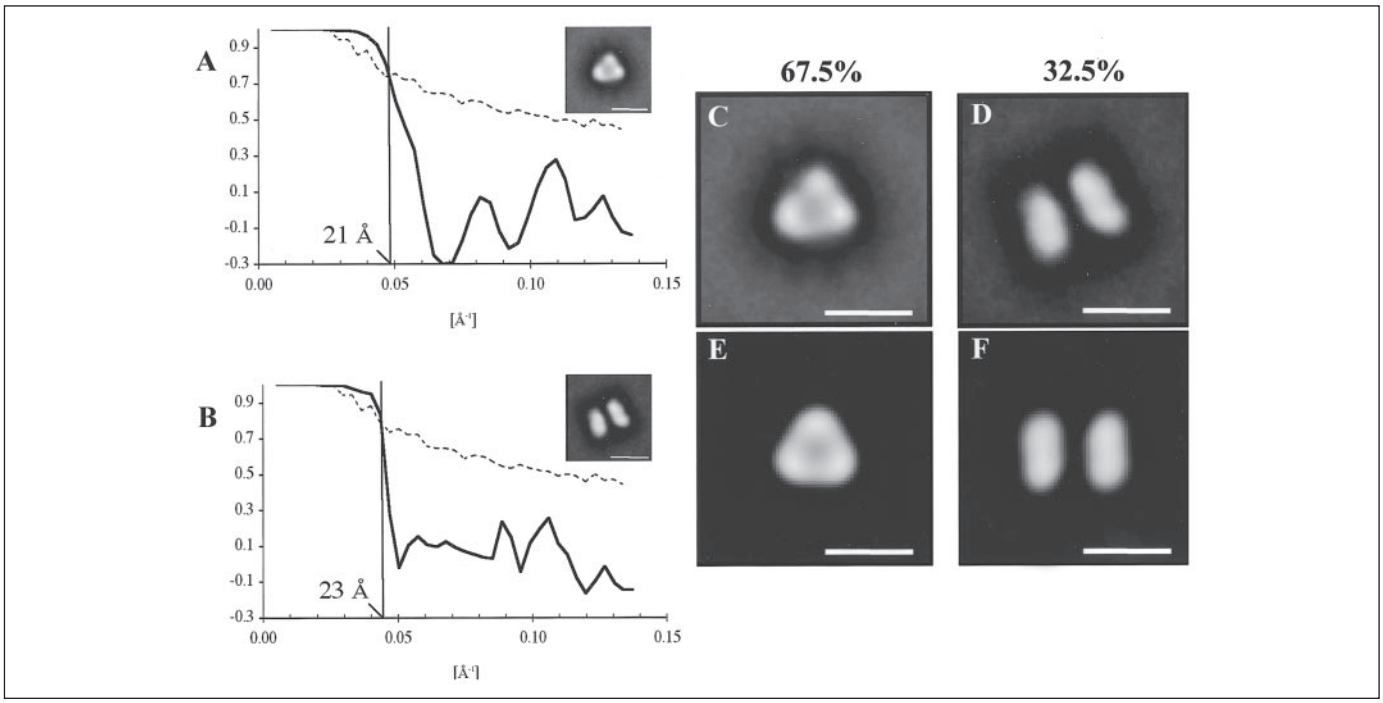


FIGURE 5. **Fourier ring correlation of averaged particles.** The respective data sets were split into two groups and compared. The resolution was calculated with a cutoff criterion of five times noise correlation of 21 (*A*) and 23 Å (*B*). *Scale bar*, 10 nm. *C* and *D* represent two-dimensional averages of single particles showing two different orientations of the protein, face on view (*C*) and side view (*D*). 3350 and 1600 particles were averaged for *C* and *D*, respectively. *E* and *F* are the same as *C* and *D*, except with 3- or 2-fold symmetry applied, respectively. *Scale bar* is 10 nm.

indicates clearly that the CaiT trimer binds detergent and lipid amounting to ~240 kDa, corresponding to ~160 DDM molecules/monomer. The formation of hexamers under normal conditions can be ruled out based on our observation of uranylacetate-induced hexamers on blue native gels (Fig. 4*C*) that were observed in the electron microscope.

Initial two-dimensional crystallization trials were carried out with *E. coli* polar lipids in various pH ranges. The vesicles thus obtained were analyzed by freeze-fracture electron microscopy, which indicated a high level of protein incorporation (data not shown). However, ordering of the protein into two-dimensional lattices was observed only at pH 7.5 or above, presumably because of pH-dependent protein-protein or lipid-protein interactions. The membranes obtained with *E. coli* polar lipids were predominantly multiple layers and poorly ordered. Through a screen for lipids, better conditions for obtaining isolated crystalline vesicles were found with choline lipids.

The vesicular two-dimensional crystals obtained with DPPC and POPC were used for electron microscopy and image processing to obtain information about the structure and the oligomeric state of the protein. The dimension of the trimer calculated from the projection map (Fig. 7) was very similar to that of the single particle, indicating a near-native structure in the detergent micelle (Fig. 5*E*).

Among the high resolution structures of the secondary transporters known, AcrB (12) and GltPh (13) are trimers. AcrB is a 12-transmembrane helix protein that uses the proton gradient to remove drugs from the cell. GltPh probably co-transports glutamate with sodium and has eight transmembrane helices. The structures of both proteins differ significantly in the arrangement of transmembrane helices and the substrate translocation pathway (12, 13). This highlights the importance of studying the structures of least one transporter from each family. In the BCCT family of secondary transporters, structural information is available only for BetP from *Corynebacterium glutamicum* at ~8 Å resolution. The projection map reveals a trimer showing densities attributed to membrane-spanning helices surrounding two less dense regions, one or both of which might be related to substrate translocation (32). We found that CaiT, a homologue of BetP, is also a trimer with similar dimensions indicated by the two-dimensional crystals.

From the structures of AcrB and GltP (12, 13), it is evident that each monomer in these trimeric membrane transporters harbors a single translocation channel. We believe that this will also be true for CaiT and BetP. A single translocation pore on the 3-fold axis of the trimer, with equal contributions from all three monomers, seems unlikely. So far, a corresponding arrangement has been found only in the ion channels, which have 4-fold symmetry. If each monomer of the BCCT transporters harbors its own independent transport pathway, this raises the question as to why they need to be trimers. There are two possible explanations. An oligomeric assembly might be required for functional cooperativity between subunits or allosteric regulation of the transport process, as has been shown for LacS (10) and proposed for anion exchanger (11). The oligomeric structure may also be required for the formation of an aqueous vestibule on the membrane surface, in which substrates are collected prior to passage through the individual monomers, as suggested for $Glt_{ph}$ (13). Alternatively, the trimer might be required simply for the correct folding and stability of the protein in the membrane.

It is striking that many, if not most, membrane proteins are found as oligomers in the membrane, whereas a functional cooperativity between subunits is rarely evident. This may suggest that the oligomers form for reasons of protein stability or perhaps to adapt to the tight space and packing constraints in the membrane. In many cases, these oligomeric assemblies of membrane proteins are stable enough to withstand the solubilization of the membrane with detergent. Further functional and structural studies are required to address the question as to why oligomers of CaiT and other transport proteins form in the membrane and how they work.

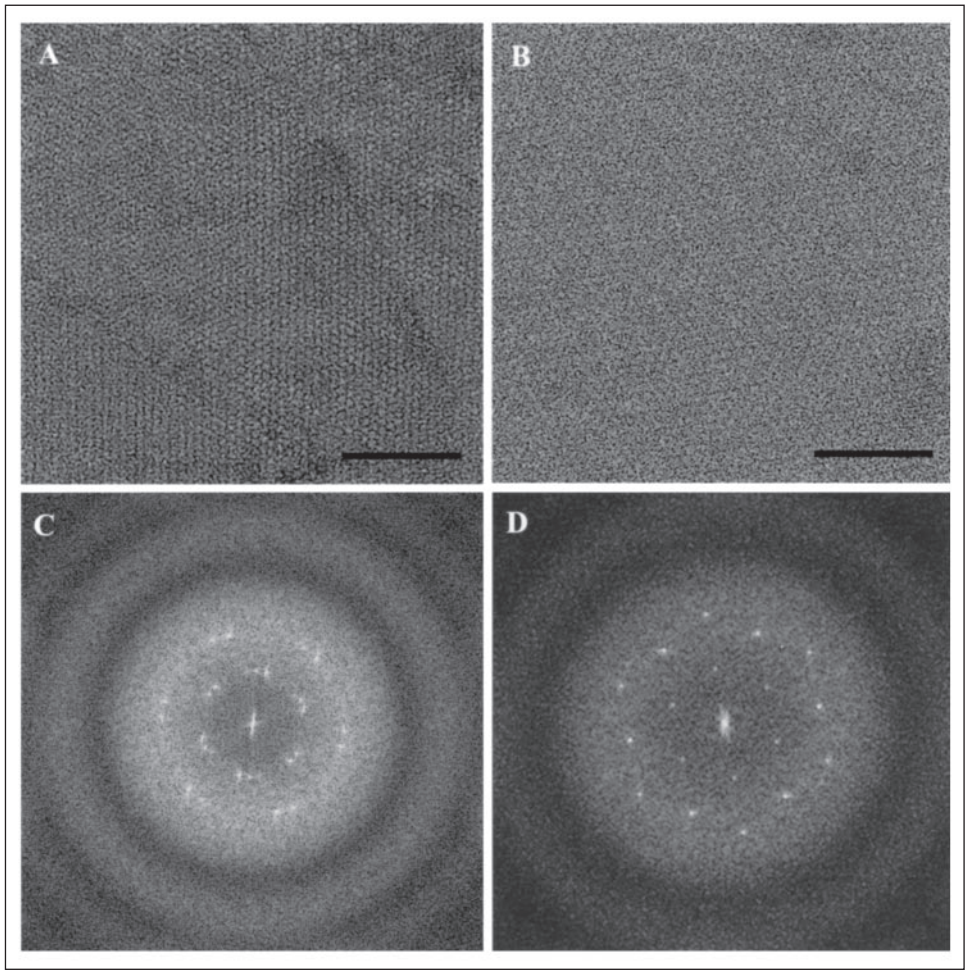


FIGURE 6. **Two-dimensional crystallization of CaiT.** Shown are two-dimensional crystal lattices for stacked (*A*) and single membranes (*B*). *Scale bar* is 100 nm. Power spectrum of stacked (*C*) and single membranes (*D*) are shown.

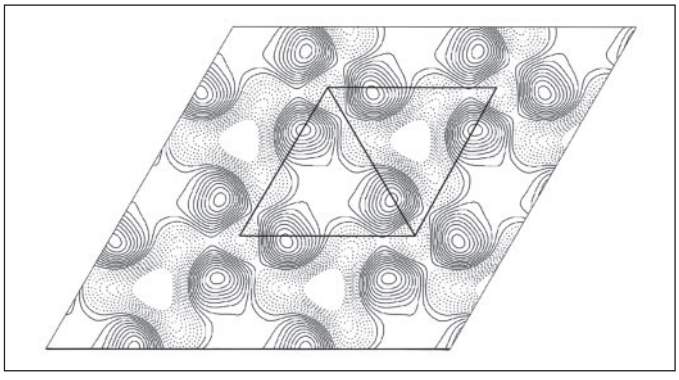

FIGURE 7. **Projection map of negatively stained two-dimensional crystals of CaiT at 25 Å with P3 symmetry applied.**

## CONCLUSIONS

The *E. coli* carnitine transporter CaiT has been produced by homologous expression on a scale of several milligrams. The purified protein was reconstituted into proteoliposomes and formed two-dimensional crystals under defined conditions. The oligomeric state of CaiT was investigated by a range of techniques. Blue native gel electrophoresis and single-particle electron microscopy indicated that the protein was a trimer, as is its homologue BetP from *C. glutamicum*. Gel filtration of CaiT indicated a size similar to apoferritin, a soluble protein with a mass of 440 kDa, confirming that this method tends to overestimate the molecular mass of membrane proteins because of bound detergent and lipid, whereas a fully denaturing SDS gel tends to underestimate it because of partial unfolding of the hydrophobic protein even by harsh detergents. The projection map calculated by the image processing of two-dimensional crystals showed a trimer of the same dimension as the single particles with dimensions similar to those of BetP. This suggests that the transporters of the BCCT family are probably trimeric. In analogy to other secondary transporters with known high resolution structures, we assume that each CaiT monomer contains one substrate translocation path. The oligomer may be required for functional cooperativity or for the stability of protein in the membrane.

## REFERENCES

1. Kramer, R., and Morbach, S. (2004) *Biochim. Biophys. Acta* **1658,** 31–36
2. Jung, H., Buchholz, M., Clausen, J., Nietschke, M., Revermann, A., Schmid, R., and Jung, K. (2002) *J. Biol. Chem.* **277,** 39251–39258
3. Jung, H., Jung, K., and Kleber, H. P. (1989) *Biochim. Biophys. Acta* (1003), 270–276
4. Veenhoff, L. M., Heuberger, E., and Poolman, B. (2002) *Trends Biochem. Sci.* **27,** 242–249
5. Abramson, J., Smirnova, I., Kasho, V., Verner, G., Kaback, H. R., and Iwata, S. (2003) *Science* **301,** 610–615
6. Huang, Y., Lemieux, M. J., Song, J., Auer, M., and Wang, D. N. (2003) *Science* **301,** 616–620
7. Ambudkar, S. V., Anantharam, V., and Maloney, P. C. (1990) *J. Biol. Chem.* **265,** 12287–12292
8. Williams, K. A., Geldmacher-Kaufer, U., Padan, E., Schuldiner, S., and Kühlbrandt, W. (1999) *EMBO J.* **13,** 3558–3563
9. Vinothkumar, K. R., Smits, S. H., and Kühlbrandt, W. (2005) *EMBO J.* **24,** 2720–2729
10. Wang, D. N., Kühlbrandt, W., Sarabia, V. E., and Reithmeier, R. A. (1993) *EMBO J.* **6,** 2233–2239
11. Mindell, J. A., Maduke, M., Miller, C., and Grigorieff, N. (2001) *Nature* **409,** 219–223

12. Murakami, S., Nakashima, R., Yamashita, E., and Yamaguchi, A. (2002) *Nature* **419,** 587–593
13. Yernool, D., Boudker, O., Jin, Y., and Gouaux, E. (2004) *Nature* **431,** 811–818
14. Veenhoff, L. M., Heuberger, E., and Poolman, B. (2001) *EMBO J.* **20,** 3056–3062
15. Casey, J. R., and Reithmeier, R. A. (1991) *J. Biol. Chem.* **266,** 15726–15737
16. Schägger, H., and Von Jagow, G. (1991) *Anal. Biochem.* **199,** 223–231
17. Frank, J., Radermacher, M., Penczek, P., Zhu, J., Li, Y., Ladjadj, M., and Leith, A. (1996) *J. Struct. Biol.* **116,** 190–199
18. Radermacher, M., Wagenknecht, T., Verschoor, A., and Frank, J. (1987) *J. Microsc.* (*Oxf.*) **146,** 113–136
19. Marco, S., Chagoyen, M., de la Fraga, L. G., and Carazo, J. M. (1996) *Ultramicroscopy* **66,** 5–10
20. Radermacher, M. (1997) *Scan Micros.* **11,** 171–177
21. Radermacher, M., Ruiz, T., Wieczorek, H., and Gruber, G. (2001) *J. Struct. Biol.* **135,** 26–37
22. Marabini, R., and Carazo, J. M. (1994) *Biophys. J.* **66,** 1804–1814
23. Marabini, R., Masegosa, I. M., San Martin, M. C., Marco, S., Fernandez, J. J., de la Fraga, L. G., Vaquerizo, C., and Carazo, J. M. (1996) *J. Struct. Biol.* **116,** 237–240
24. Henderson, R., Baldwin, J. M., Downing, K. H., Lepault, J., and Zemlin, F. (1986) *Ultramicroscopy* **19,** 147–178
25. Crowther, R. A., Henderson, R., and Smith, J. M. (1996) *J. Struct. Biol.* **116,** 9–16
26. Valpuesta, J. M., Carrascosa, J. L., and Henderson, R., (1994) *J. Mol. Biol.* **240,** 281–287
27. Heuberger, E. H., Veenhoff, L. M., Duurkens, R. H., Friesen, R. H., and Poolman, B. (2002) *J. Mol. Biol.* **317,** 591–600
28. Bessonneau, P., Besson, V., Collinson, I., and Duong, F. (2002) *EMBO J.* **21,** 995–1003
29. Gendreau, S., Voswinkel, S., Torres-Salazar, D., Lang, N., Heidtmann, H., Detro-Dassen, S., Schmalzing, G., Hidalgo, P., and Fahlke, C. (2004) *J. Biol. Chem.* **279,** 39505–39512
30. Valiyaveetil, F. I., Zhou, Y., and MacKinnon, R. (2002) *Biochemistry* **41,** 10771–10777
31. Standfuss, J., and Kühlbrandt, W. (2004) *J. Biol. Chem.* **279,** 36884–36891
32. Ziegler, C., Morbach, S., Schiller, D., Kramer, R., Tziatzios, C., Schubert, D., and Kühlbrandt, W. (2004) *J. Mol. Biol.* **337,** 1137–1147